Urol Res (2010) 38:439–452
DOI 10.1007/s00240-010-0330-1

SYMPOSIUM PAPER

Comparison of the pathology of interstitial plaque in human ICSF stone patients to NHERF-1 and THP-null mice

Andrew P. Evan · Edward J. Weinman · Xue-Ru Wu · James E. Lingeman · Elaine M. Worcester · Fredric L. Coe

Received: 6 October 2010 / Accepted: 8 October 2010 / Published online: 10 November 2010

Abstract Extensive evidence now supports the role of papillary interstitial deposits—Randall's plaques—in the formation of stones in the idiopathic, calcium oxalate stone former. These plaques begin as deposits of apatite in the basement membranes of the thin limbs of Henle's loop, but can grow to become extensive deposits beneath the epithelium covering the papillary surface. Erosion of this covering epithelium allows deposition of calcium oxalate onto this plaque material, and the transition of mineral type and organic material from plaque to stone has been investigated. The fraction of the papilla surface that is covered with Randall's plaque correlates with stone number in these patients, as well as with urine calcium excretion, and plaque coverage also correlates inversely with urine volume and pH. Two animal models—the NHERF-1 and THP-null mice—have been shown to develop sites of interstitial apatite plaque in the renal papilla. In these animal models, the sites of interstitial plaque in the inner medulla are similar to that found in human idiopathic calcium oxalate stone formers, except that the deposits in the mouse models are not localized solely to the basement membrane of the thin limbs of Henle's loop, as in humans. This may be due to the different morphology of the human versus mouse papillary region. Both mouse models appear to be important to characterize further in order to determine how well they mimic human kidney stone disease.

Keywords Randall's plaque · Transmission electron microscopy · Histopathology · Endoscopy

Proceedings paper from the 3rd International Urolithiasis Research Symposium, Indianapolis, Indiana, USA, December 3-4, 2009.

A. P. Evan (✉)
Department of Anatomy and Cell Biology,
Indiana University School of Medicine,
635 Barnhill Drive, MS 5055S, Indianapolis,
IN 46223, USA
e-mail: evan@anatomy.iupui.edu

E. J. Weinman
Department of Medicine and Physiology,
University of Maryland, School of Medicine,
Baltimore, MD, USA

X.-R. Wu
Departments of Urology and Pathology,
New York University School of Medicine,
New York, NY, USA

X.-R. Wu
New York Harbor Healthcare System,
Manhattan Campus, New York, NY, USA

J. E. Lingeman
Methodist Hospital for Kidney Stone Disease,
Indiana University School of Medicine, Indianapolis, IN, USA

E. M. Worcester · F. L. Coe
University of Chicago School of Medicine, Chicago, IL, USA

Introduction

While the precise mechanisms for kidney stone formation are not entirely clear, there is a recognition that crystals must be retained in the kidney if a stone is to grow to a size that will generate clinically relevant symptoms. There are three primary hypotheses in the field of kidney stone disease that explain stone formation and growth [1]. First, stones form on sites of interstitial plaque called Randall's plaque, usually at the papillary tip as a overgrowth and as such are attached to the papilla; second, small crystalline deposits form by attaching to the apical cell surface of lining cells of the distal nephron and third, stones form as free-floating objects in the urinary space.

The primary focus of this paper will be on the first hypothesis that being the role that sites of interstitial plaque play in stone formation. Alexander Randall is credited with the discovery of calcified material in the interstitium of selected stone formers [2, 3]. His studies were performed on 1,154 kidneys examined after autopsy with just a hand lens. He noted a cream-colored area near the tip of the renal papilla, and beneath the urothelium, suburothelial in location, in a total of 227 kidneys (or 19.6%). On microscopic examination and staining, the cream-colored areas were found to be composed of calcium salts deposited in the interstitial space of the renal papilla around tubules, as apposed to actually being in tubular lumens. Randall called these sites of calcium plaque, papillary lesions type I. In addition, he found evidence of very limited cellular destruction and round-cell infiltration, meaning that there was limited evidence of inflammation or tissue injury in these kidneys. He reasoned that such changes are inevitable findings at the autopsy table and believed that they represented a secondary factor from pre-existing pathological conditions and not a primary process of stone disease. Randall also found some areas of black material about 1 mm in diameter on a site of suburothelial plaque. When Randall performed microscopic examination of this black material and the plaque associated with it, he noted a region of interstitial plaque denuded of an urothelial covering with the black-colored material attached to the exposed plaque. This black material was later determined to be the earliest evidence of a renal stone. In addition, he discovered visible calcium plaque supporting a stone, which projected into the lumen of the minor calyx. Thus, the microscopic site of the black-colored material appeared to be acting as a nidus for future crystal deposition and the slow growth of a kidney stone. A total of 65 kidneys were found to have one or more stones attached to the renal papilla at sites of calcium plaque. Chemical analysis of the sites of calcium plaque and associated stone found the calcium plaque to be composed of calcium carbonate and phosphate while the stones varied from calcium phosphate for the smallest stones to calcium oxalate in the larger stones.

Despite these clear and precise observations of Randall, his hypothesis did not change the direction of the kidney stone research. Instead, multiple levels of criticism challenged his most basic findings and his studies were set aside as interesting but probably not relevant. First, it was argued that all forms of stone disease appeared to fit the attached stone idea. Randall unfortunately made the decision to try to fit all stone formation to one hypothesis. Others discovered small sites of interstitial plaque in non-stone formers as well as stone formers and concluded that probably all renal papilla have some regions of interstitial plaque [4–7] and suggested that sites of Randall's plaque are not unique to kidney stone formers [8–10].

It was Stoller et al. [11] that reinvestigated the idea of Randall's plaque using high-resolution radiography of cadaveric kidneys. Their first study showed that sites of Randall's plaque were not merely suburothelial in location, but extended deep within the papilla and were associated with the tubular segments and vessels of the papilla. Because only 2 of the 50 consecutive autopsies had clinical evidence of stone disease, they were not able to determine if there was a link between papillary calcification and the pathogenesis of stones. It was Stoller's next two studies [12, 13] using endoscopic techniques that provided strong evidence in support of Randall's original observations. The highest incidence of plaque was with calcium oxalate stones and the lowest incidence with cystine stones. They also found a positive trend between hypercalciuria and increasing plaque severity but no correlation of any stone risk factor with patient age or gender.

The purpose of this paper is twofold, first to review the literature on relevant studies on Randall's plaque in human kidney stone formers and second to determine if there is an animal model that closely mimics the human data. New observations on the NHERF-1 null mouse will be presented and those findings will be compared with the published findings in the THP-null mouse.

Randall's plaque only in ICSF patients

Pattern of Randall's plaque in ICSF patients

It was the recent studies of Stoller [11–13] that motivated our team to design a new experimental approach to determine for ourselves if the hypothesis that Randall's plaque, calcium phosphate deposits in kidneys of patients with calcium renal stones, arise in unique anatomical regions of the kidney, their formation conditioned by specific stone-forming pathophysiologies. To test this hypothesis, we performed intraoperative biopsies of plaque in kidneys of idiopathic calcium stone formers and non-stone formers after nephrectomy using state-of-the-art endoscopic, microscopic, and metabolic techniques.

Although we have now studied ten different groups of stone formers and carefully phenotyped each group, only the idiopathic calcium oxalate stone formers (ICSF) patients [14] will be reported in this paper. To date, we have studied 30 ICSF patients [15, 16] each fulfilling the following criteria: had at least one stone analyzed showing to be composed of calcium oxalate, and no stones containing uric acid, struvite, cystine, or over 50% calcium phosphate; and had none of the systemic disorders such as primary hyperparathyroidism, sarcoidosis, vitamin D excess, hyperthyroidsim, or renal tububar acidosis. Compared with controls, the ICSF patients had higher urinary

calcium levels, and supersaturations with respect to calcium oxalate and calcium phosphate.

During percutaneous nephrolithotomy (PNL) performed for stone removal, each papilla was video recorded with a digital endoscope for future mapping studies, and selected papilla [15] were biopsied at sites of Randall's plaque or just adjacent to these regions. Figure 1a illustrates a papilla from an ICSF patient showing multiple brownish colored stones attached to the papilla tip at sites of irregular, whitish lesions beneath the papillary side of the stones. These stones were removed individually for stone analysis and the underlying region of Randall's plaque was biopsied and stained by the Yasue method for the localization of calcium salts. Figure 1b shows a low-power image of a section through the entire face of such a biopsy with the papillary tip at the bottom of the section. The dark blue-brownish stained material represents sites of calcium deposits. These deposits are located exclusively in the interstitial space with no evidence of crystals in tubular lumens and the mineral extends from the papillary tip toward the junction of the outer and inner medulla. No evidence of cellular injury or inflammation was noted. To determine the progression of these mineral deposits, we carefully studied biopsies obtained in adjacent regions of obvious sites of Randall's plaque. Such an area is seen in Fig. 2a. The first site that we were able to detect mineral deposition was in the basement membranes of the thin limbs of Henle's loop. The deposits appear as small spherical structures outlining the tubular basement membrane with extensions developing into the nearby interstitial space (arrow). Transmission electron microscopy (Fig. 2b) revealed that the crystalline deposits were spherical in shape and were as small as 50 nm. Their internal features varied from a uniform electron-dense appearance to a multi-laminated structure with alternating light (crystal) and dark (matrix) layers up to 6–7 in number (arrowheads). As areas with denser amounts of deposits were examined, the interstitial deposits ranged from single spheres to large collections that appeared to coalesce into islands of plaque and matrix material (Fig. 3a–d). In the interstitial space, single deposits were seen associated with type 1 collagen bundles (insert 3b). As the density of the plaque increased, it was seen to invade the basement membrane of nearby collecting ducts and vasa recta as well

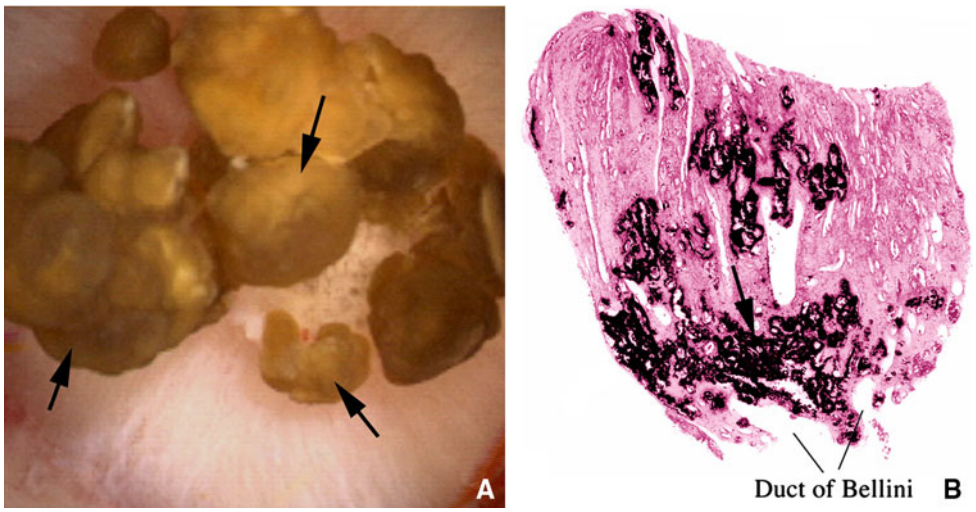

Fig. 1 Endoscopic and histological image of papilla from idiopathic calcium oxalate stone former. **a** Numerous stones (*arrows*) attached to a site of Randall's plaque. Histopathologic examination of the area seen in **a** and stained with Yasue method shows a *black–brown* material (*arrow*) in the interstitial space

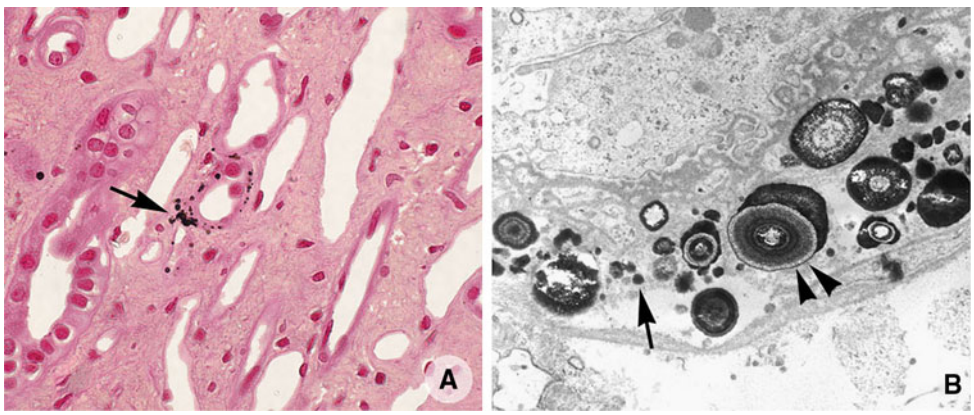

Fig. 2 Light and electron microscopic images of sites of interstitial plaque. By light microscopy **a** small, *black–brown*, *spherical* deposits (*arrow*) are noted in the basement membrane of the thin loops of Henle. By transmission electron microscopy **b** individual deposits (*arrows*) characterized by their spherical shape and multi-laminar interior are easily noted while embedded in the basement membrane material

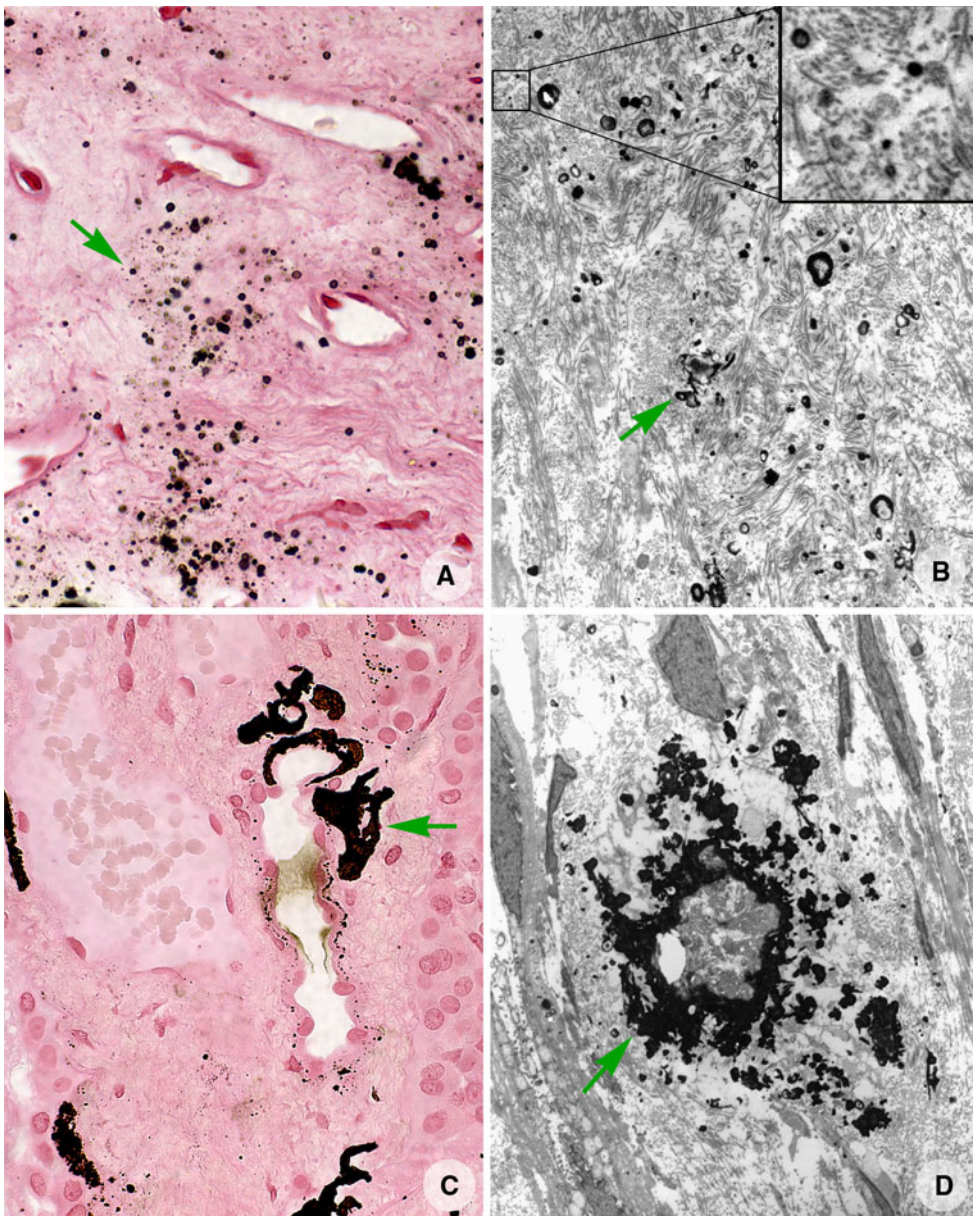

Fig. 3 Light and electron microscopic images of sites of interstitial plaque as it advances in the interstitium. **a** and **c** are light microscopic images showing the accumulation of interstitial deposits (*green arrows*) while **b** and **d** are transmission electron micrographs showing the close association of the deposits with collagen bundles (see *inset* **b**)

as surrounding interstitial cells (Fig. 4a, b) without damaging these cells. Eventually, these dense islands of mineral are found positioned beneath the basal surface of the urothelium (Fig. 4c) and thus can be seen as a suburothelial whitish region during endoscopy.

Molecular structure of interstitial deposits

In order to understand the detailed structural makeup of these individual crystalline deposits (Fig. 5a), a series of studies were designed to determine if two proteins involved in crystal formation were present in Randall's plaque. First, osteopontin, a well-defined crystal-associated urine protein, was localized using immunohistochemistry and immunoelectron microscopy. By immunoelectron microscopy, osteopontin gold labeling was found mainly on the surfaces of apatite crystals, at the junction of the crystal/organic layer (Fig. 5b) [17]. A similar immunogold labeling pattern was seen in the islands of interstitial plaque. The second protein studied was inter-α-trypsin inhibitor (IαI) because of its association with calcium oxalate matrix and its effectiveness as an inhibitor of calcium oxalate crystallization. IαI is a glycoprotein in which two heavy chains (H1 & H2) are covalently linked to bikunin via a chondroitin sulfate bridge. There is a pre-α trypsin inhibitor molecule that contains bikunin bound to heavy chain 3 (H3). Our study [18] only found the heavy chain 3 localized to the individual deposits and only in the matrix layers of these microspherical (Fig. 5c). Diffuse immunoelectron gold labeling of H3 was noted in the islands of interstitial plaque

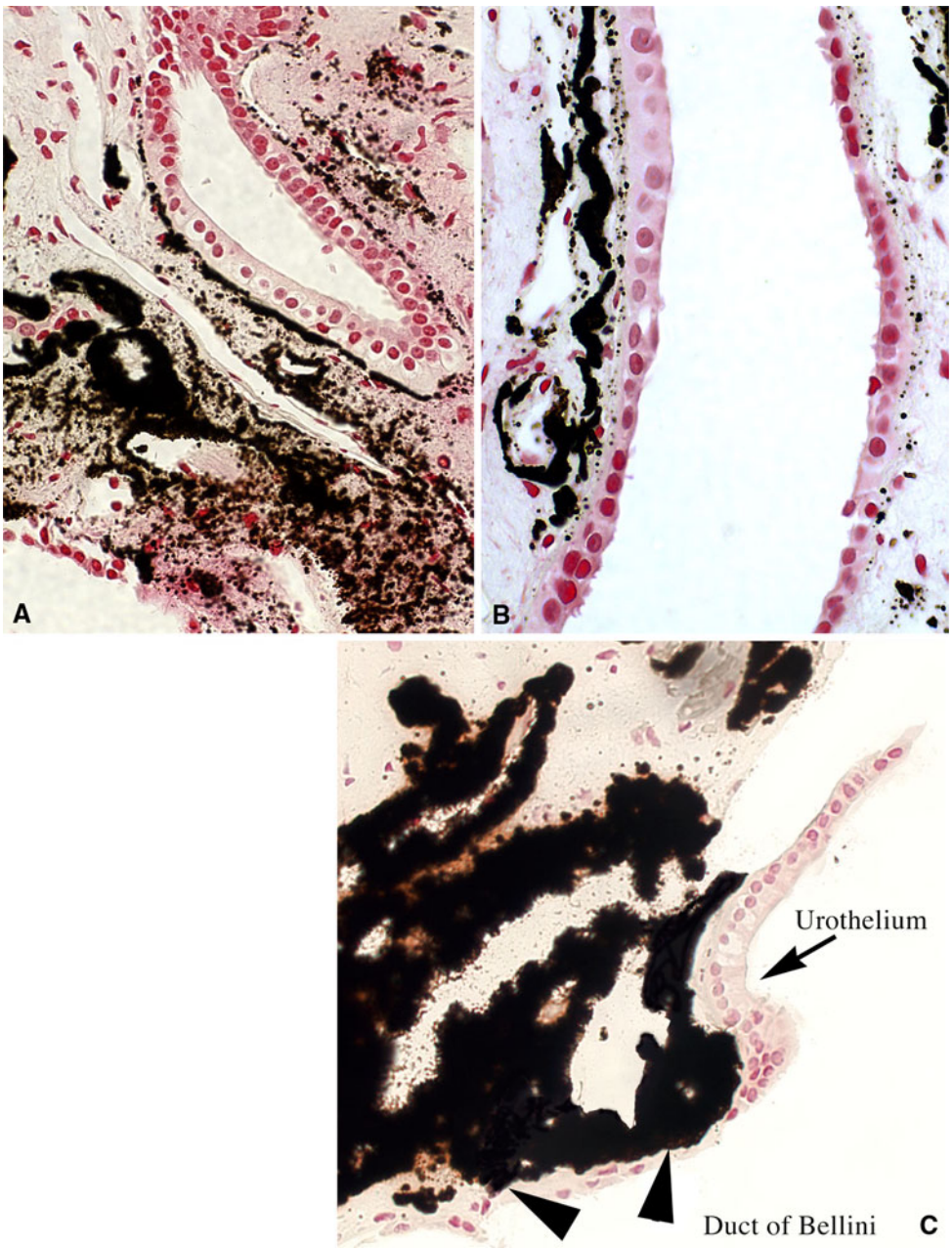

Fig. 4 Massive accumulation of interstitial deposits. **a**, **b** Large regions of interstitial deposits surrounding not only the thin loops of Henle but also nearby inner medullary collecting ducts. The deposits collect at the basal surface of the urothelium forming a dense mat of material (*arrowheads*)

along with osteopontin. The data from the osteopontin and inter-α-trypsin inhibitor molecules clearly show that at least two of the well-known proteins involved in apatite crystallization are also integral to interstitial plaque formation.

Stone overgrowth on interstitial plaque

Since 1937, it has been apparent that calcium oxalate stones often grow attached to the renal papilla and specifically to areas of the papilla containing interstitial apatite deposits [2]. Both Randall [2, 3] and Anderson [19] published light microscopic images showing continuity between sites of interstitial plaque and the papillary side of a kidney stone. However, they were not able to detail the morphological features of this plaque-stone interface or perform mineral composition studies. Therefore, our group performed en bloc biopsies of very small stones (Fig. 6a, b) so that we could show the anatomy and microstructure of the plaque-stone interface [20]. Figure 6c shows a light microscopic view of the tissue within the region of interstitial plaque beneath the stone that detached during the demineralization process. Clearly, the region of papilla related to the deep side of the stone (asterisk) was denuded of urothelial cells and was continuous with a mineral layer in the stone at an attachment site. Transmission electron microscopic examination of the plaque–stone interface

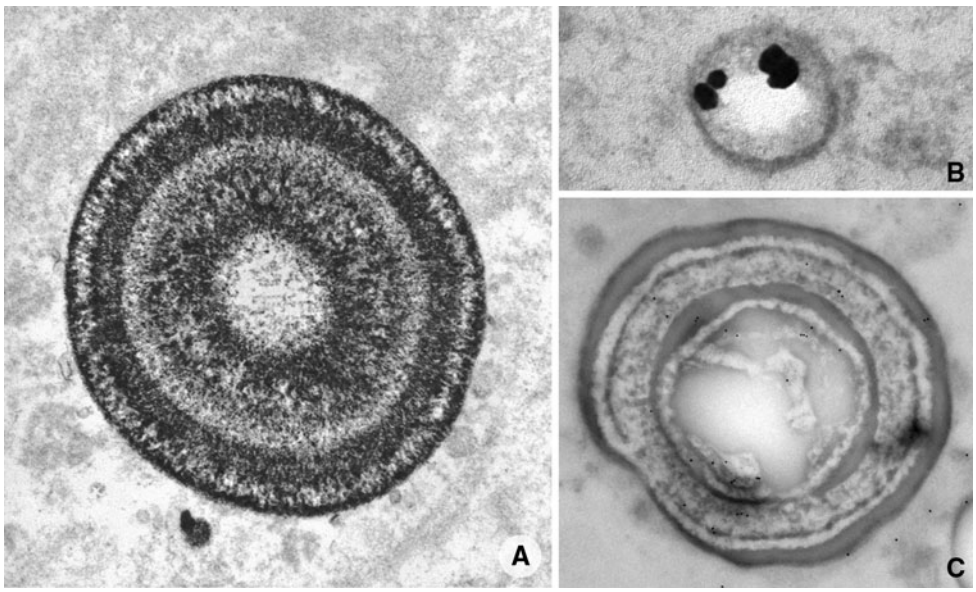

Fig. 5 Individual deposits seen by transmission electron microscopy. **a** The multilayer appearance of the interstitial deposits of alternating electron dense and lucent layers. **b** The location of osteopontin (*dark black circles*) while **c** shows the location of heavy chain three of the inter-alpha-trypsin inhibitor molecule

(Fig. 7) reveals that the exposed plaque is covered by a dark ribbon-like layer (Fig. 7A) and alternating laminae of crystal (white in figure) and black organic material arranged in nine separate layers (see insert of Fig. 7). In the thickest of the white laminae one can see tiny, thin spicules that run perpendicular to the surface and have the appearance of multiple voids that contained tightly packed crystals (small arrows). At the outer surface of the ribbon, crystals extend from rafts in the ribbon (large arrows and asterisk). All crystals were surrounded and covered by a matrix-like material.

Plaque abundance and metabolic correlates

Because renal papillary interstitial (Randall's) plaques are common in calcium stone formers, we hypothesized that plaque should increase directly with urine calcium excretion and inversely with urine volume [21]. In order to determine the accuracy of our hypotheses, we measured papillary plaque areas on video images collected at the time of PNL from both idiopathic calcium oxalate stone formers and non-stone formers and examined 24-h urine data to identify significant correlations. Figure 8a presents mean plaque coverage of papillae from the non-stone formers and ICSF patients. Although interstitial plaque is present in non-stone formers (0.6%), the amount is significantly smaller than that measured in the ICSF patients (7.6%). Twenty-four hour urine samples collected at times random and remote from the surgery showed a strong positive correlation of plaque abundance with urine calcium excretion and strong negative correlations with urine volume and pH (Fig. 8b). Although we have no information about ion compositions in the interstitial microenvironment where plaque forms, we have new data showing that there is reduced calcium reabsorption at the proximal tubule in ICSF patients [22]. This could result in an increased delivery of calcium into the thick ascending limb with reabsorption of calcium without water into the outer medullary tissue. Because of the presence of nearby vas recta in the outer medulla, the counter current mechanism would more than likely cause the interstitial calcium concentration in the outer medulla to exceed that of blood. Descending vas recta could then load calcium into the interstitial space within the inner medulla by a vas wash down mechanism causing the calcium concentration to greatly increase. The presence of a high calcium level and possibly phosphate level could lead to a physiochemical formation of plaque in the inner medulla at sites of the thin limbs of Henle's loop.

Stone formation and plaque abundance

In a separate study, we examined papillary plaque coverage as a function of duration of their stone disease and number of stone events [23]. Figure 9a–c shows separate endoscopic views of three ICSF patients. The upper image shows a papilla from an ICSF patient that has had only one stone event, and a short duration of stone disease of 0.17 years. Plaque area is 1.7%. The middle image shows a papilla from an ICSF patient that has had two stone events and a moderate length of stone disease (5 years), with a plaque area of 12.4%. The lower panel shows a papilla from an ICSF patient that has had seven stone events and 30 years of kidney stone disease and a

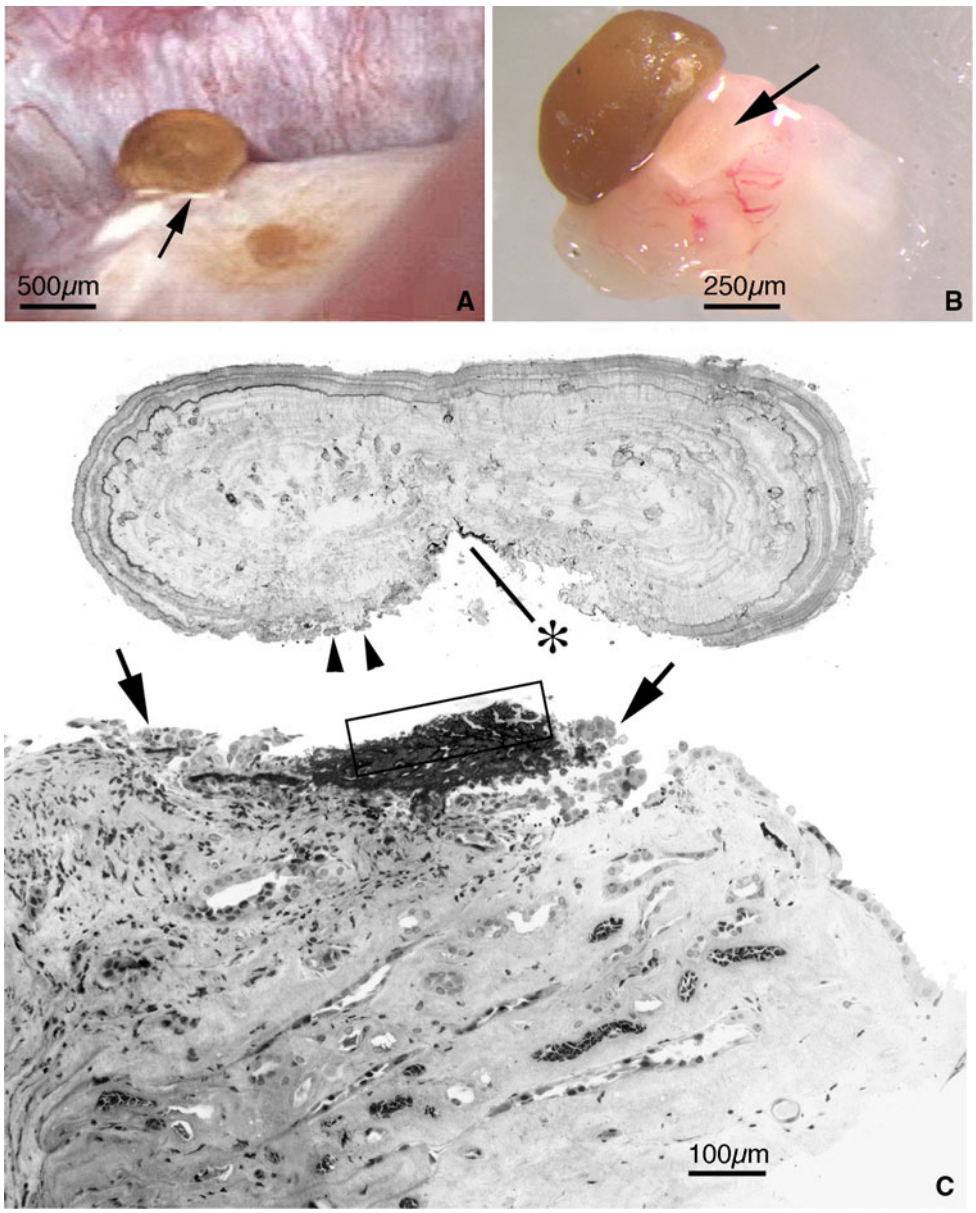

Fig. 6 Endoscopic and light microscopic images of individual stone with associated interstitial tissue still attached. **a** An endoscopic image of a small stone attached to a site of interstitial plaque (*white area* pointed out by an *arrow*). **b** Same stone and tissue after biopsy. The stone-tissue complex was decalcified, sectioned for light microscopy and illustrated in **c**. The stone is seen above a *dark* region in the tissue (*rectangle*), which is interstitial plaque. A portion of plaque is noted at the base of the stone (see *asterisk*). The *arrows* mark the sites where the urothelium is lost. The *double arrowheads* point out a region of cellular debris

plaque area of 27.4%. Next we plotted stone number against log 10 mean plaque surface area and number of stones against plaque time score (Fig. 9d). The strongest correlation was between number of stones plotted against plaque time score. These positive results support the contention that plaque is essential for calcium stone formation.

Animal models of Randall's plaque

Mechanisms for Randall's plaque formation

Our extensive investigation of papillary biopsies from now ten different stone-forming groups strongly suggests that sites of Randall's plaque are essential for stone formation and growth in ICSF patients. In fact, it would appear that if we could eliminate the formation of Randall's plaque in these patients, we could prevent their stones from forming. These conclusions have driven us to determine the mechanism responsible for Randall's plaque formation. To date, we have tested the hypothesis that there is a cell-mediated process responsible for Randall's plaque formation. It states that kidney interstitial cells transdifferentiate into osteoblasts in ICSF patients, thereby initiating a cell-mediated process of bone-like formation in the interstitium which leads to interstitial plaque formation. We hypothesized an osteoblast-like activity in the inner medulla of ICSF patients because of the known multipotential interstitial cells located in the inner medulla

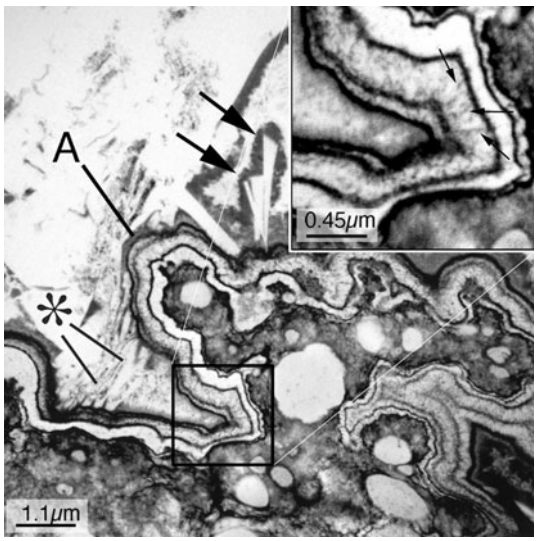

Fig. 7 Transmission electron micrograph showing the plaque-stone interface. The *lower right corner* of the figure is papillary tissue filled with interstitial plaque while the *upper left corner* is urinary space. Separating the interstital plaque from the urinary space is a ribbon-like structure. It is formed from multiple electron-dense and -lucent layers (see *inset* at *upper right*). Crystals of various sizes and coated with matrix material are seen inserting into the ribbon-like structure at a region labeled *A*

and the generous amount of type one collagen at the papillary tip, the site of interstitial plaque formation. Preliminary results from our investigation of this hypothesis was presented at the last IKSI meeting and showed that osteoblast-like activity could not be identified in ICSF biopsies [24].

Our negative findings on the cell-mediated hypothesis and our new observations of reduced proximal tubule calcium reabsorption in ICSF patients have led us to hypothesize a new mechanism for interstitial plaque formation termed the vas wash-down theory. As the increased calcium load leaves the proximal tubule it will be transported out of the thick ascending limb without water into the interstitial space of the outer medulla. A series of small blood vessels called vas recta in the renal medulla aid in a counter current mechanism to permit the concentration of ions as fluid moves from the outer medulla to the inner medulla. In ICSF patients, calcium levels in the outer medulla may exceed that of blood permitting the wash-down of calcium by way of vas recta into the interstitial space of the inner medulla. This increased calcium concentration in the inner medulla could then drive the papillary interstitium to crystallize a calcium phosphate

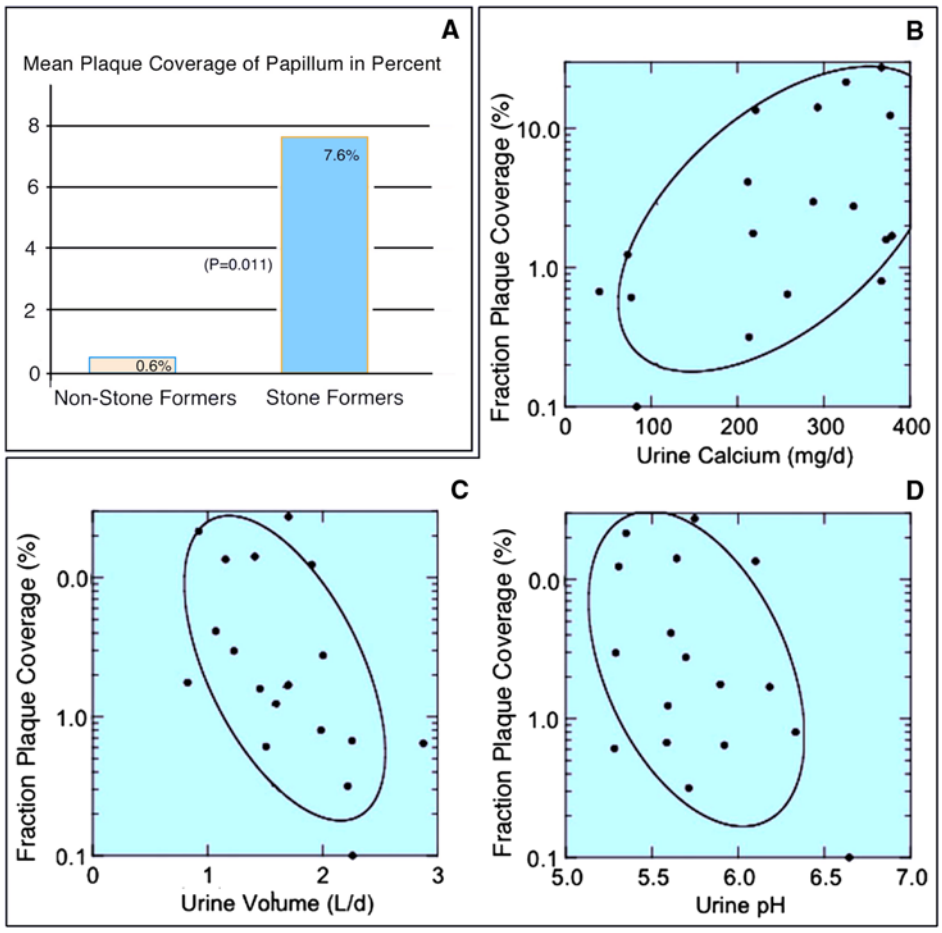

Fig. 8 **a** The mean plaque coverage for papillium in percent for non-stone-formers versus idiopathic calcium oxalate stone formers while **b**, **c**, and **d** show the relationship of urinary calcium, volume, and pH to plaque coverage

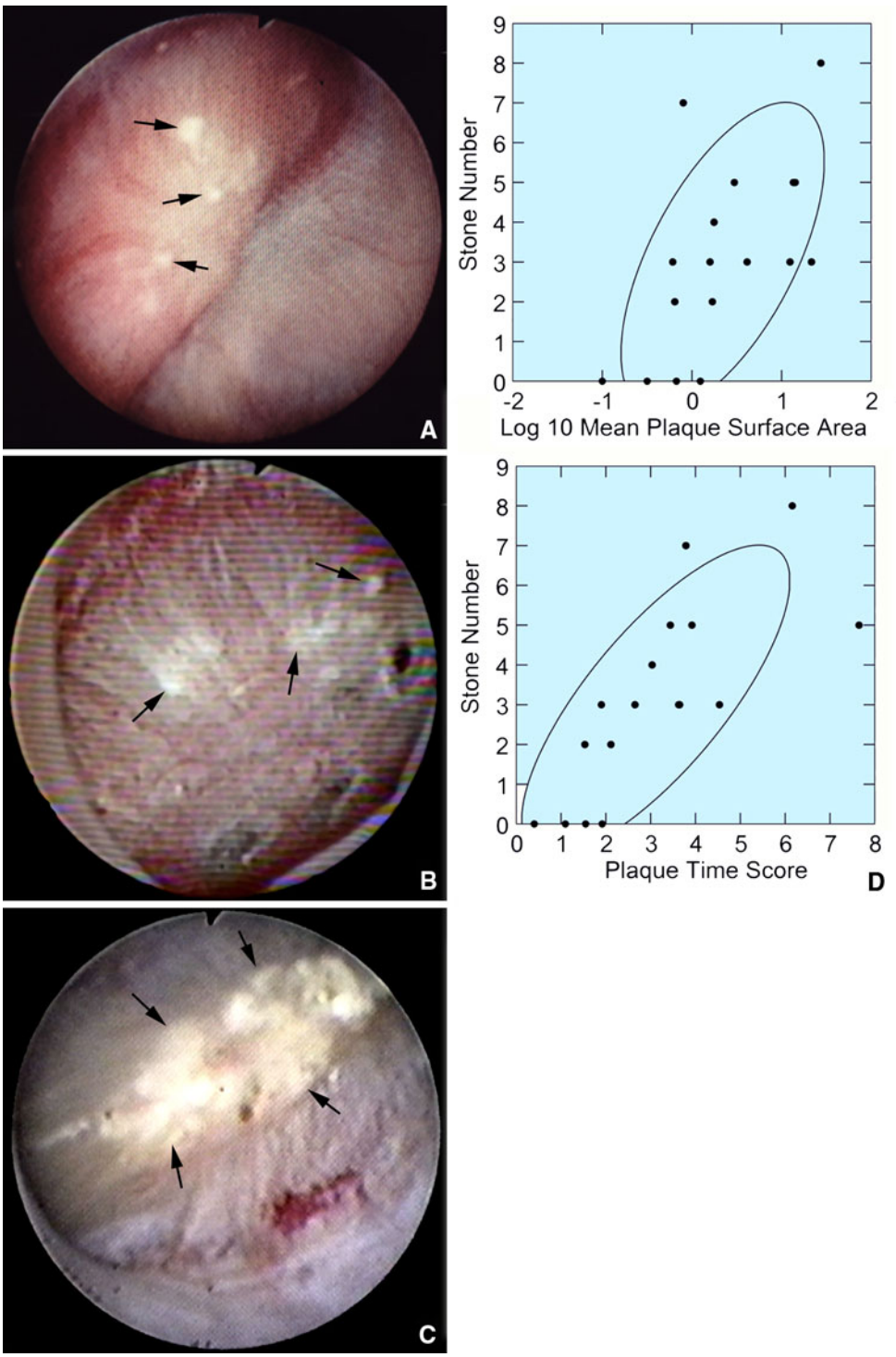

Fig. 9 Variation in amount of Randall's plaque between papilla (**a**–**c**) and relationship of stone number to mean plaque surface area (**d**) and plaque time score (**d**)

product like interstitial plaque on a collagen matrix by simple physiochemical processes. To test such a hypothesis, we need an animal model that mimics the formation of interstitial plaque seen in ICSF patients. Therefore, we have been examining a number of mouse and rat models for the presence of interstitial plaque in the papillary interstitum. Two animal models will be highlighted in this paper: the NHERF-1 null mouse and OPN KO mouse.

The NHERF-1 null mouse

The sodium–hydrogen exchanger regulatory factor, NHERF (NHERF-1), is a protein adapter that is highly expressed in epithelial cells. It was isolated initially as a necessary cofactor in cAMP-associated inhibition of the renal brush border sodium–hydrogen exchanger (NHE3) [25], and it was shown to be involved with the apical

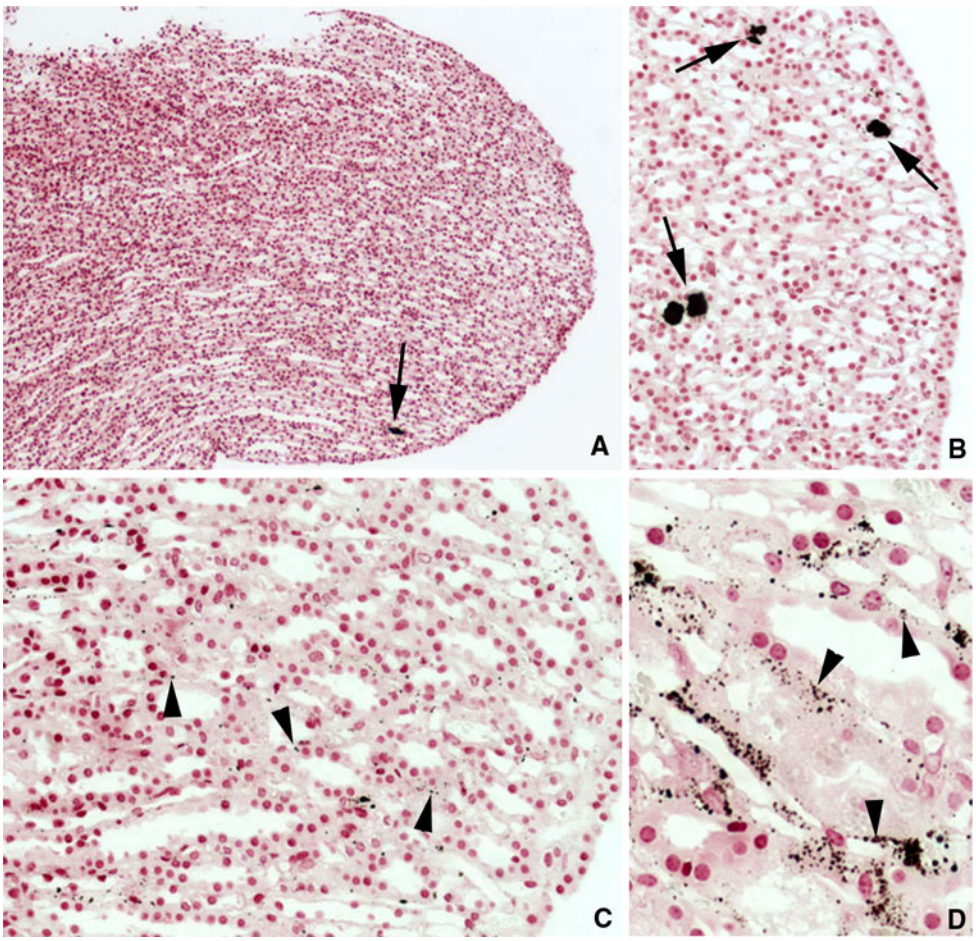

Fig. 10 Light microscopic image of interstitial plaque in 17-month-old NHERF-1 mouse. **a**, **b** A few large areas of interstitial deposits (*arrows*) near the papillary tip. At higher magnifications, numerous small *black–brown* spherical deposits (*arrows*) are noted in the basement membranes of the thin loops of Henle and inner medullary collecting ducts

targeting of Npt2a (NaP1 IIa). NHERF-1 was later shown to be identical to ezrin-binding protein 50 (EBP50). The NHERF protein contains two tandem PDZ domains and a C-terminal sequence that binds several members of the ERM (ezrin–radixin–moesin) family of membrane-cytoskeletal adapters. Wild-type mouse proximal tubules strongly express NHERF-1 in the brush border membranes in association with NHE3, Npt2a and ezrin [26]. Npt2a is responsible for the reabsorption of $\sim$80% of the phosphate filtered at the glomerulus, and its abundance in the kidney brush border membrane increases in response to restriction of the dietary intake of phosphate and decreased in response to PTH [27].

In addition to regulation of NHE3, NHERF is involved in the localization/turnover of several proteins, including G-protein coupled receptors, platelet-derived growth factor receptor, ion transporters, NaPi cotransporter, Na/HCO3 cotransporters, and calcium channels [28]. NHERF also recruits non-membrane proteins such as YAP-65, members of the phospholipase C-beta family, and the GRK6A protein kinase to the apical membrane of cells, and this recruitment can be related to regulation of cell functions and the response of the cell to membrane signals [28].

In 2002 Weinman et al. [29] generated a NHERF-1 knockout mouse model, which showed decreased brush-border membrane Npt2a expression and increased expression of Npt2a in intracellular vesicles of proximal tubules. These animals also showed phosphate wasting, decreased bone mineral content, and failure to adapt to phosphate deprivation. In order to determine if these changes were age-related, they examined male and female wild-type and NHERF-1 null mice from 12 to 54 weeks of age. Young male and female NHERF-$1^{-/-}$ mice had hypercalciuria, hyperphosphaturia, hyperuricosuria, but normal urine volumes. They showed higher vitamin D levels and their PTH levels tended towards a decrease with altered apical PTH receptor as compared with wild-type mice. The 6-month-old NHERF-1 null mice showed a correction in their phosphate/creatinine ratio in that the NHERF-1 and wild-type animals had a similar phosphate/creatinine ratio. At 1 year of age, the NHERF-1 null mice still showed hypercalciuria and hyperuricosuria. Histological examination of the papillary tissues from these animals was performed to determine the presence of mineral deposits because the sustained increases in the urinary excretions of calcium and uric acid suggested that these functional changes might favor the formation of kidney stones.

Interstitial deposits were noted primarily in the 54-week-old NHERF-1 null mice, though an occasional deposit was noted in the wild-type controls. However, the density of deposits in the NHERF-1 null mice was small compared with the large field of interstitial deposits observed in ICSF human stone formers. The interstitial location of mineral deposits in the NHERF-1 null mouse kidney is very different from that described in Npt2a mice where the mineral is intraluminal along the entire nephron [30]. These observations led to the design of a study where we examined the kidneys from even older NHERF-1 null mice with the idea that the deposits would gradually increase in amount as a function of the animal's age.

Kidneys were harvested from two female- and one male wild-type mice of approximately 17 months of age and two female- and two male NHERF-1 knockout mice approximately 17–19 months of age. All kidneys were fixed in 10% buffered formalin and embedded in paraffin for light microscopic examination. Serial sections were cut at 7 μm and stained with the Yasue method to detect sites of calcium deposits per our previous publications [15]. When the Yasue-stained sections from the wild-type animals were examined, an occasional Yasue-positive deposit of about 15–25 μm was noted in the papillary interstitium. However, in the NHERF-1 null mice, numerous Yasue-positive deposits were found in the interstitial space of the renal medulla. Deposits were never observed in the cortex. The deposits were distributed in two size groups. The first type of deposit was large in size (<10 μm) but few in number (Fig. 10a, b) and was located in the interstitial space near thin loops of Henle and inner medullary collecting ducts. The second type of deposit was numerous but very small in size (<2 μm) surrounding and within the basement membranes of both thin loops of Henle and inner medullary collecting ducts (Fig. 10c, d). The majority of the deposits were located in the interstitial space near the papillary tip. No detectable cellular changes were noted in the nearby lining cells of the thin loops of Henle or the inner medullary collecting duct or any evidence of acute or chronic interstitial inflammation/fibrosis at sites of the deposits (Fig. 10a–d).

Although the age of the animals studied in these experiments was about 6–8 months older than the animals Weinman et al. [25] originally reported on, there did not seem to be a noticeable increase in the amount of interstitial deposits between the two reports suggesting that age is not the key factor for the accumulation of the deposits. The rather low amount of deposits detected also indicates that there might not be enough interstitial plaque to drive attached stone formation as noted in the human ICSF studies. The initial location of the deposits in the NHERF-1 null mice was not exclusive to the basement membranes of the thin loops of Henle as we reported in the ICSF patients but was equally localized to the basement membranes of the inner medullary collecting ducts and thin loops of Henle. This difference in deposit location may relate to the reduced interstitial space in the inner medulla of the mouse compared with a much larger papillary interstitium in the human kidney.

The THP-null mouse

Tamm-Horsfall protein (THP), also called uromodulin, is a kidney-specific, heavily glycosylated protein generated by cells of the thick ascending limb and has been strongly implicated in kidney stone formation. It is abundant in the matrix of human calcium oxalate (CaOx) stones, has been shown to inhibit the aggregation of both CaOx and calcium phosphate (CaP) crystals [31], is reduced in the urine of kidney stone formers [32], and has a lower level of sialic acids than that of healthy individuals [33]. As a means to better understand the role of THP in kidney stone disease, THP knockout models have been recently generated in two different laboratories. The THP-null mice created by Bates et al. [34] does not form any type of crystal or stones in the kidney when followed up to 3 years; however, the THP-null mice created by Wu et al. [35] show crystalline deposits in the renal medulla as early as 2–3 months of age

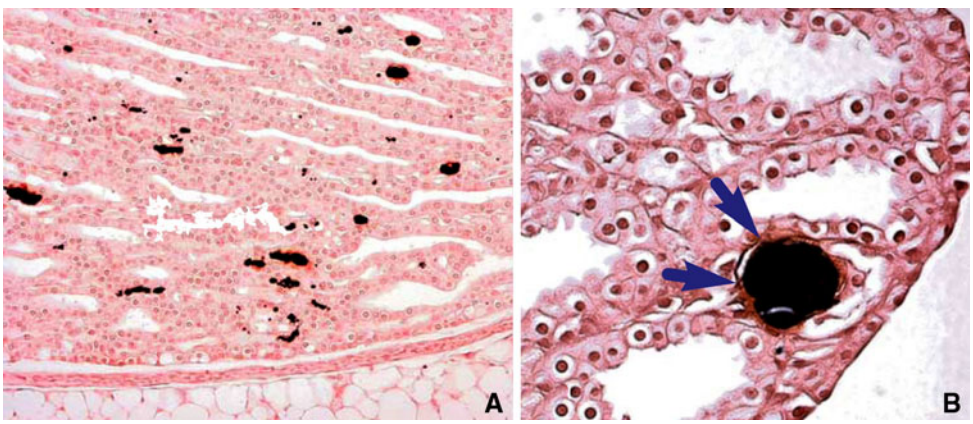

Fig. 11 Light microscopic image of interstitial plaque in 5-month-old THP-null mouse. **a** Multiple *black–brown* interstitial deposits near the papillary tip while **b** shows a single interstitial deposit (*arrows*) in an inner medullary collecting duct

with less than 20% possessing papillary interstital deposits (Fig. 11a). However, there was an occasional site of intra-luminal deposits in the inner medullary collecting ducts (Fig. 11b). By 5–8 weeks, about 50% of the THP-null animals possessed interstitial deposits and that number increased to 88% by 15 months (Fig. 12a–d). Transmission electron microscopy showed that the sites of interstitial deposits were spherical in shape with multiple layers of alternating electron dark to lucent (Fig. 13a, b), a pattern identical to that described for human idiopathic calcium oxalate stone formers. However, the deposits were not localized to the basement membranes of the thin loops of Henle but were found surrounding the inner medullary collecting ducts as frequently as they were to the thin loops of Henle. Rarely was an intra-luminal deposit noted at the later time points. The mineral type was consistently hydroxyapatite. The mineral type was independent of genetic background, gender, and THP gene dosage.

Twenty-four-hour urine values of male THP-null 5–8-month animals showed a reduced urine volume (also a third of the wild type animals showed this change). Reduced urinary creatinine, oxalate and citrate levels, lower urine pH (6.0 vs. 6.4 for wild type), and increased magnesium levels suggested a possible loop defect. The animals appeared volume depleted. These urinary changes resemble human ileostomy kidney stone formers with reduced urine volume and an acidic pH [36].

Thus the interstitial deposits of THP-null animals have the same morphology of the human idiopathic calcium oxalate stone formers as well as having the same mineral type. However, the THP-null animals also possess intra-luminal deposits and a very different urinary chemistry.

In conclusion, the two animal models, the NHERF-1 and THP-null mice, clearly develop sites of interstitial apatite plaque in the renal papilla with the NHERF-1 animal showing the greater amount of deposits. The sites of interstitial plaque in the inner medulla is similar to that found in human idiopathic calcium oxalate stone formers; however, the deposits in the mouse models are not localized to the basement membrane of the thin loops of Henle as is Randall's plaque in humans. This may be due to the different morphology of the human versus mouse papillary region. Functionally, the two animal models are very different from each other. The NHERF-1 mouse may represent a defect in the proximal tubule resulting in reduced calcium reabsorption like human idiopathic calcium oxalate stone

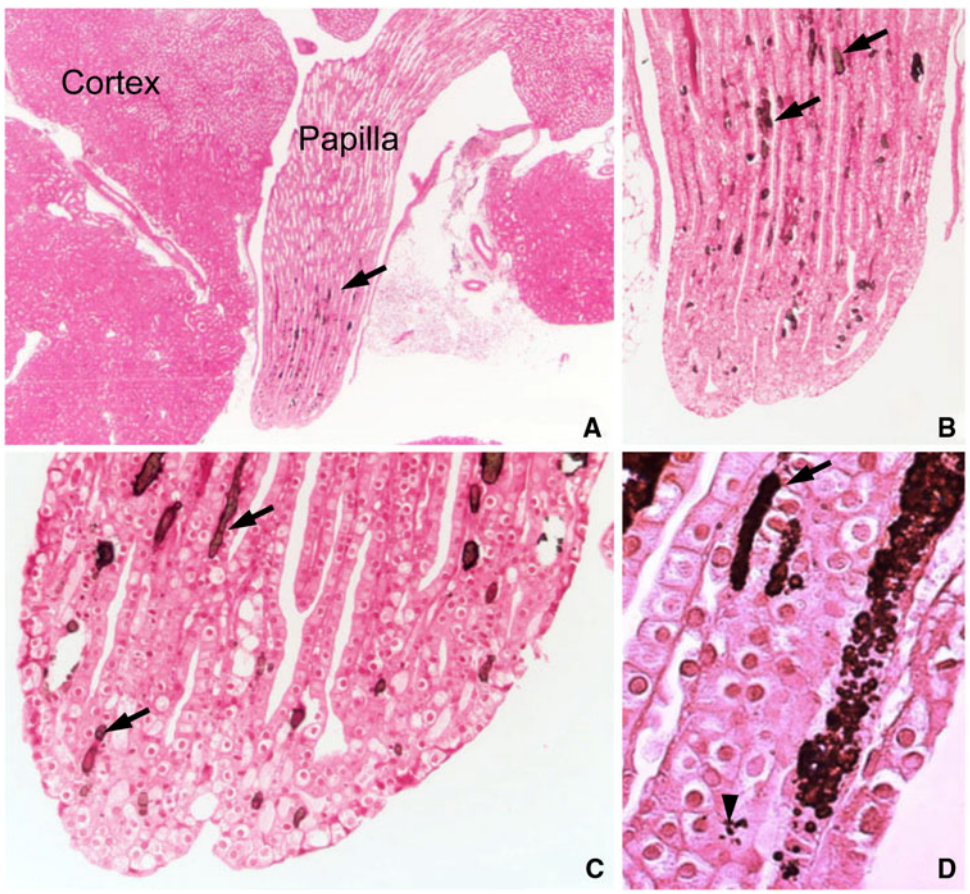

Fig. 12 Light microscopic image of interstitial plaque in 15-month-old THP-null mouse. **a** A low-magnification light micrograph showing the entire papilla and the multiple sties of interstitial deposits (*arrow*). **b** The same papilla in **a** at a higher magnification, note the numerous sites of interstitial deposits (*arrows*). This same papilla is seen at progressively higher magnifications in **c** and **d**

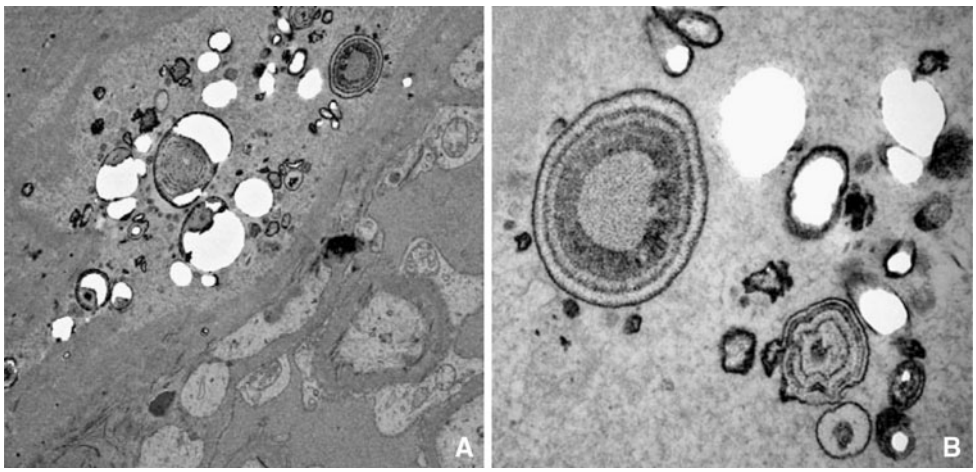

Fig. 13 Transmission electron micrograph of interstitial deposits. At low magnification, **a** the plaque particles are spherical in shape and multilayered. At a higher magnification, the deposits from this THP-null mouse look identical to that seen in human idiopathic calcium oxalate stone formers (Fig. 5a)

formers. The THP-null mouse may have a distal tubular defect and thus mimics ileostomy patients with low urine volumes and acidic urine. Both models appear to be important to characterize further in order to determine how well they mimic human kidney stone disease.

Acknowledgment This study was funded by NIH P01 DK56788.

References

1. Coe FL, Evan AP, Worcester EM, Lingeman JE (2010) Three pathways for human kidney stone formation. Urol Res 38(3):147–160
2. Randall A (1937) The origin and growth of renal calculi. Ann Surg 105:1009–1027
3. Randall A (1940) The etiology of primary renal calculus. Int Abst Surg 71:209–240
4. Burry AF, Axelsen RA, Trolove P, Sallis JD (1976) Calcification in the renal medulla: a classification based on a prospective study of 2261 necropsies. Hum Pathol 7:435–449
5. Haggit RC, Pitcock JA (1971) Renal medullary calcifications: a light and electron microscopic study. J Urol 106:342–347
6. Vermooten V (1942) The origin and development in the renal papilla of Randall's calcium plaques. J Urol 48:27–31
7. Anderson LMJR (1946) Origin, frequency and significance of microscopic calculi in kidney. Surg Gynecol Obstetr 82:275–282
8. Khan SR, Finlayson B, Hackett R (1984) Renal papillary changes in patient with calcium oxalate lithiasis. Urology 23:194–199
9. Cooke SAR (1970) The site of calcification in the human renal papilla. Br J Surg 57:890–896
10. Weller RO, Nester B, Cooke SAR (1971) Calcification in the human papilla: an electron-microscope study. J Pathol 107:211–216
11. Stoller ML, Shami GS, McCormick VD, Kerschmann RL (1996) High resolution radiography of cadaveric kidneys: unraveling the mystery of Randall's plaque formation. J Urol 156:1263–1266
12. Low RK, Stoller ML (1997) Endoscopic mapping of renal papillae for Randall's plaque in patients with urinary stone disease. J Urol 158:2062–2064
13. Low RK, Stoller ML, Schreiber CK (2000) Metabolic and urinary risk factors associated with Randall's papillary plaque. J Endourol 14:507–510
14. Coe FL, Parks JH, Asplin JR (1992) The pathogenesis and treatment of kidney stones. N Engl J Med 327:1141–1152
15. Evan AP, Lingeman JE, Coe FL, Parks JH, Bledsoe SB, Shao Y, Sommer AJ, Paterson RF, Kuo RL, Grynpas M (2003) Randall's plaque of patients with nephrolithiasis begins in basement membranes of thin loops of Henle. JCI 111:607–616
16. Evan AP, Coe FL, Gillen D, Lingeman JE, Bledsoe S, Worcester EM (2008) Renal intra-tubular crystals and hyaluronan staining occur in stone formers with bypass surgery but not with idiopathic calcium oxalate stones. Anat Rec 291:325–334
17. Evan AP, Coe FL, Rittling SR, Bledsoe SM, Shao Y, Lingeman JE, Worcester EM (2005) Apatite plaque particles in inner medulla of kidneys of calcium oxalate stone formers: osteopontin localizaton. Kidney Intl 68:145–154
18. Evan AP, Bledsoe S, Worcester EM, Coe FL, Lingeman JE, Bergsland KJ (2007) Renal inter-α-trypsin inhibitor heavy chain 3 increases in calcium oxalate stone-forming patients. Kidney Intl 72:1503–1511
19. Anderson WAD (1944) Renal calcification in adults. J Urol 44:29–34
20. Evan AP, Coe FL, Lingeman JE, Shao Y, Anderson JC, Worcester EM (2007) Mechanism of formation of human calcium oxalate renal stones on Randall's plaque. Anat Rec 290:1315–1323
21. Kuo RL, Lingeman JE, Evan AP, Paterson RF, Parks JH, Bledsoe SB, Munch LC, Coe FL (2003) Urine calcium and volume predict coverage of renal papilla by Randalls plaque. Kidney Intl 64:2150–2154
22. Worcester EM, Bergsland K, Evan AP, Parks JH, Coe FL, Willis LR, Clark DL, Gillen D (2008) Evidence for increased postprandial distal nephron calcium delivery in hypercalciuric stone forming patients. AJP 295:F1286–F1294
23. Kim SC, Tinmouth WW, Coe F, Kuo RL, Paterson RF, Parks J, Evan AP, Lingeman JL (2005) Stone formation is proportional to papillary surface coverage by Randall's plaque. J Urol 173:117–119
24. Evan AP, Bledsoe SB (2008) Bone genes in the kidney stone former. In: Evan AP, McAteer JA, Lingeman JE, Williams JC (eds) Renal stone disease. Proceedings of the second international urolithiasis research symposium. American Institute of Physics, Melville, pp 33–43
25. Weinman EJ, Sreplock D, Shenolikar S (1995) Characterization of a protein co-factor that mediates protein kinase A regulation of the renal brush border membrane Na^+-H^+ exchanger. J Clin Invest 95:2143–2149
26. Wade JB, Liu J, Coleman RA, Cunningham R, Steplock DA, Lee-Kwon W, Pallone TL, Shenolikar S, Weinman EJ (2003) Localization and interaction of NHERF isoforms in the renal proximal tubule of the mouse. APJ 285:C1494–C1503

27. Murer H, Hernando N, Forster I, Biber J (2003) Regulation of Na/Pi transporter in the proximal tubule. Annu Rev Physiol 65:51–542
28. Voltz JW, Weinman EJ, Shenolikar S (2001) Expanding the role of nherf, a pdz-domain containing protein adapter, to growth regulation. Oncogene 20(44):6309–6314
29. Shenolikar S, Voltz JW, Minkoff CM, Wade JB, Weinman EJ (2002) Targeted distrution of the mouse NHERF-1 gene promotes internalization of proximal tubule sodium-phosphate cotransporter type IIa and renal phosphate wasting. Proc Natl Acad Sci 99:11470–11475
30. Chau H, El-Maadawy S, McKee MD, Tenenhouse HS (2003) Renal calcification in mice homozygous for the disrupted type IIa Na/Pi cotransporter gene Npt2. J Bone Miner Res 18:644–657
31. Kumar V, Lieske JC (2006) Protein regulation of intrarenal crystallization. Curr Opin Nephrol Hypertens 15:374–380
32. Lau WH, Leong WS, Ismail Z, Gam LH (2008) Qualification and application of an ELISA for the determination of Tamm Horsfall Protein (THP) in human urine and its use for screening of kidney stone disease. Int J Biol Sci 4:215–222
33. Knorle R, Schnierle P, Koch A, Buchholz NP, Hering F, Seiler H, Ackermann T, Rutishauser G (1994) Tamm-Horsfall glycoprotein: role in inhibition and promotion of renal calcium oxalate stone formation studied with Fourier-transform infrared spectroscopy. Clin Chem 40:1739–1743
34. Raffi H, Baes JM, Laszik Z, Kumar S (2006) Tamm-Horsfall protein knockout mice do not develop medullary cystic kidney disease. Kidney Intl 69:1914–1915
35. Liu YL, Mo L, Goldfarb DS, Evan AP, Liang F, Khan SR, Lieske JC, Wu, X-R (2010) Progressive renal papillary calcification and ureteral stone formation in mice deficient for tamm-Horsfall protein. AJP. doi:10.1152/ajprenal.00243.2010
36. Evan AP, Lingeman JE, Coe FL, Bledsoe SB, Sommer AJ, Williams JC Jr, Krambeck AE, Worcester EM (2009) Intratubular deposits, urine and stone composition are divergent in patients with ileostomy. Kidney Int 76:1081–1088